JOURNAL OF APPLIED PHYSICS VOLUME 84, NUMBER 3 1 AUGUST 1998

# Phase separation and ordering in InGaN alloys grown by molecular beam epitaxy

D. Doppalapudi[a] and S. N. Basu
*Department of Manufacturing Engineering, Boston University, Boston, Massachusetts 02215*

K. F. Ludwig, Jr. and T. D. Moustakas[b]
*Department of Electrical and Computer Engineering and Department of Physics, Boston University, Boston, Massachusetts 02215*

(Received 25 March 1998; accepted for publication 30 April 1998)

In this study, we investigated phase separation and long-range atomic ordering phenomena in InGaN alloys produced by molecular beam epitaxy. Films grown at substrate temperatures of 700–750 °C with indium concentration higher than 35% showed phase separation, in good agreement with thermodynamic predictions for spinodal decomposition. Films grown at lower substrate temperatures (650–675 °C) revealed compositional inhomogeneity when the indium content was larger than 25%. These films, upon annealing to 725 °C, underwent phase separation, similar to those grown at the same temperature. The InGaN films also exhibited long-range atomic ordering. The ordering parameter was found to increase with the growth rate of the films, consistent with the notion that ordering is induced at the growth surface. The ordered phase was found to be stable up to annealing temperatures of 725 °C. A competition between ordering and phase separation has been observed, suggesting that the driving force for both phenomena is lattice strain in the alloy. © *1998 American Institute of Physics.* [S0021-8979(98)05815-0]

## I. INTRODUCTION

The traditional method of tailoring the electrical and optical properties of III-V compounds is through the formation of solid solutions between the corresponding binary compounds. In such mixed compounds, the tetrahedral radii of the atomic species occupying a particular sublattice may be different from each other. The resulting strain in the layers could lead to deviations from homogeneity of the sublattice. Zunger and Mahajan have reviewed several observations which indicate that when the tetrahedral radii are different, two types of structural variations are observed: phase separation and atomic ordering.[1] Extensive transmission electron microscopy (TEM) investigations with selective area diffraction (SAD) and dark field imaging have been reported that reveal phase separation as well as long-range atomic ordering in these compounds.[2–5] Both these phenomena are believed to be two dimensional in nature, occurring on the growth surface and being subsequently trapped in the bulk due to kinetic limitations. Atomic ordering in these compounds is caused by surface-reconstruction induced subsurface stresses which force preferential occupation of sites by atomic species of different radii.[3] In most of the atomic ordering observations, the epitaxial growth was carried out on [100] oriented substrates with zinc blende structures.

In recent years, the InGaN ternary system has attracted special interest because of its potential for the formation of light emitting devices operating in the red to ultraviolet region of the energy spectrum. Several designs of double heterostructures (DHs), single quantum well (SQW) and multi-quantum well (MQW) structures using InGaN active layers have been successfully grown and processed to make light emitting diodes (LEDs) and laser diodes (LDs).[6–9] In spite of all these developments, the growth and properties of InGaN alloys have yet to be completely optimized or understood.

The difficulties in InGaN growth are mainly due to (a) very high equilibrium vapor pressures (EVPs) of nitrogen over InN and (b) a large lattice mismatch (11%) between InN and GaN. At the standard growth temperatures of GaN by molecular beam epitaxy (MBE) (750 °C), the EVP of InN is more than ten orders of magnitude greater than that of GaN.[10] Thus, indium has a very low sticking coefficient at typical growth temperatures for GaN by MBE and the temperature has to be reduced significantly to prevent dissociation of InN. However, at lower temperatures, indium droplets may form, which act as sinks for InN and prevent incorporation of higher indium fractions in the film.[10,11] In addition, the crystalline quality of the film is inferior at lower temperatures due to poor surface mobility of the ad-atoms, resulting in three-dimensional growth. Furthermore, the large lattice mismatch between InN and GaN (due to the very different tetrahedral radii) results in highly strained InGaN alloys. Therefore, at relatively low growth temperatures (650–800 °C), phase separation is a major concern.

The majority of the III-V ternary and quaternary alloys are predicted to be thermodynamically unstable and show a tendency towards clustering and phase separation.[1,12–14] Stringfellow[12] developed the delta lattice parameter (DLP) model for III-V compounds with zinc blende structure, to calculate the critical temperature ($T_c$) above which a particular ternary or quaternary system is completely miscible. The model is based on the correlation between the immiscibility

[a]Electronic mail: dharani@engc.bu.edu
[b]Electronic mail: tdm@bu.edu

 © 1998 American Institute of Physics

Downloaded 22 May 2002 to 128.197.57.187. Redistribution subject to AIP license or copyright, see http://ojps.aip.org/japo/japcr.jsp

and the difference in the lattice parameters of the components, and assumes that Vegard's law of solid solutions is applicable. However, there have been very few studies on the InN–GaN quasi-binary system and even fewer reports on phase separation in this system. Singh *et al.*[15] applied the DLP model using the lattice parameters of the zinc blende structures of InN and GaN and found that the critical temperature ($T_c$) above which the InN–GaN system is completely miscible is 2457 K. Ho and Stringfellow used a modified valence-force-field (VFF) model and calculated a much lower $T_c$ of 1473 K.[16] Since even this temperature is much higher than typical growth temperatures of InGaN alloys, phase separation is expected in these alloys based on thermodynamic considerations.

Based on x-ray diffraction (XRD) and optical absorption studies, Singh and co-workers[15,17,18] provided strong evidence of phase separation in InGaN thick films grown by MBE. More recently, other researchers reported phase separation in thick InGaN films grown by metalorganic chemical vapor deposition (MOCVD).[19,20] Some researchers have also reported evidence of such phase separation in the form of quantum-dotlike structures in SQWs and MQWs.[21] In this article, we present studies of phase separation and long-range atomic ordering made on two sets of InGaN films: (a) those grown at relatively high temperatures (700–750 °C) and (b) films grown at lower temperatures (650–675 °C). Furthermore, we will discuss the effect of post-growth annealing on phase separation and ordering.

## II. EXPERIMENTAL METHODS

Bulk $In_xGa_{1-x}N$ films were grown on *C*-plane and *A*-plane sapphire substrates by a three-step process similar to GaN growth.[22] Sapphire substrates were first nitridated by exposing their surface to an electron cyclotron resonance (ECR) activated nitrogen plasma at 800 °C. This step was followed by the deposition of a low temperature GaN buffer of 200–300 Å thickness at 550 °C. The InGaN films were grown in the temperature range of 650–725 °C, to a thickness of 0.5–1 $\mu$m. In one of the samples investigated, the InGaN film was grown on a thick GaN film (3000 Å). By varying the fluxes of group III elements, the growth rate of the investigated films was varied from 5 to 20 Å/min. The structures of the films were characterized by reflection high energy electron diffraction (RHEED), scanning electron microscopy (SEM), XRD and TEM measurements. The XRD studies were carried out on a four-circle diffractometer using Cu $K\alpha$ radiation, monochromated by the (111) reflection of a germanium single crystal, which does not allow the $\lambda/2$ harmonic of the x-ray beam. The $In_xGa_{1-x}N$ alloy composition was determined by calculating the lattice spacing from the (0002) Bragg reflection peak which was calibrated with reference to the sapphire peak, assuming that Vegard's law is applicable for the InN–GaN system. The *d* spacings for the (0002) Bragg reflections of pure InN and pure GaN were taken to be 5.7 and 5.18 Å, respectively. The calculated indium compositions were further confirmed by energy dispersion spectra (EDS) in a SEM. TEM studies were carried out in a JEOL 2000FX electron microscope using a cold stage at 100 K, minimizing the evaporation of indium from the InGaN film.

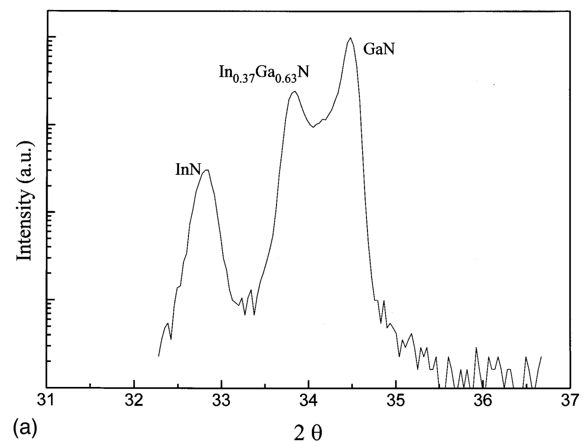


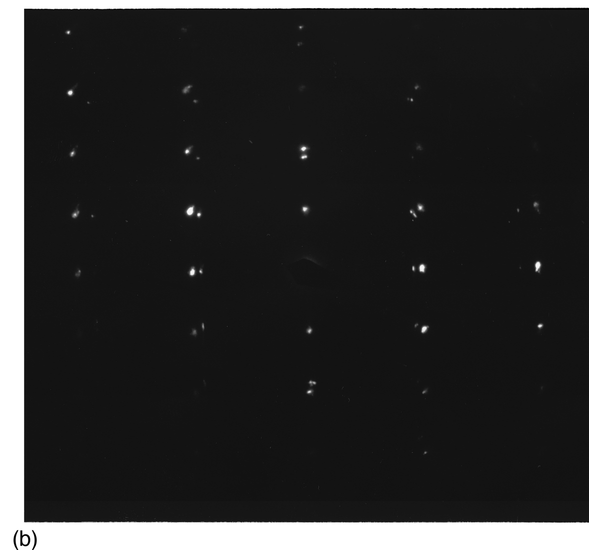


FIG. 1. (a) X-ray diffraction pattern from an InGaN film with 37% indium. (b) Cross-sectional SAD pattern along the [11-20] zone axis from the $In_{0.37}Ga_{0.63}N$ film, showing two sets of superimposed diffraction patterns from InN and InGaN.

## III. RESULTS AND DISCUSSION

The nucleation and growth of the InGaN films were monitored *in situ* by RHEED observations. The RHEED patterns were streaky and sharp, indicating good crystallinity of the surface. SEM studies showed the films to be smooth with specular surfaces, confirming the RHEED observations. However, microscopic structural studies by TEM and XRD revealed very interesting features as discussed below.

### A. Phase separation

First, we discuss the $In_xGa_{1-x}N$ films grown at relatively higher temperatures (725–750 °C). Evidence of phase separation in such films (with $x>0.35$) grown on thick GaN films has been presented earlier, based on XRD and optical absorption studies.[15,17,18] Figure 1(a) is an XRD pattern of an InGaN film with 37% (atomic) indium, grown at 725 °C. A strong phase separated InN peak is clearly seen. The InGaN film in this case was grown on a thick (3000 Å) GaN film. In

Downloaded 22 May 2002 to 128.197.57.187. Redistribution subject to AIP license or copyright, see http://ojps.aip.org/japo/japcr.jsp

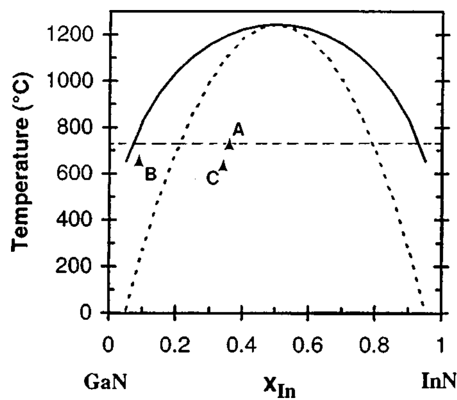


FIG. 2. Phase diagram of InN–GaN quasi-binary system (Ref. 16). The data points A, B, and C describe the three samples.

these data, a strong $In_{0.37}Ga_{0.63}N$ peak is also seen, as the phase separation was incomplete due to kinetic limitations. Figure 1(b) is a TEM SAD pattern from the cross-sectional view of the same film, viewed along the [11-20] zone axis, clearly showing the presence of more than one phase in the material. The inter-planar spacings corresponding to the two sets of superimposed diffraction patterns were calculated using calibration from the sapphire diffraction pattern taken under identical conditions. These values correspond to lattice parameters of $In_{0.97}Ga_{0.03}N$ and $In_{0.37}Ga_{0.63}N$ compositions, respectively. This gives direct evidence of phase separation in bulk InGaN alloys. The same result was confirmed by SAD studies from the plan-view of the same film, taken at the [0001] zone axis. Dark field images taken in plan and cross-sectional views showed features with sharp contrast in the lattice, which could be due to phase separated InN. Recently, El-Masry *et al.* reported a similar ''tweed'' appearance in InGaN films grown by MOCVD with In$\sim$49%,[20] and attributed it to spinodal decomposition.

The observed phase separation is evidently driven by strain due to the mixing of the two lattice mismatched components of the InGaN alloy system. Indium atoms are excluded from the InGaN lattice to form an alloy of a different composition and reduce the strain energy of the system. As discussed earlier, based on thermodynamic considerations, InN and GaN are immiscible at these growth temperatures. From the phase diagram calculated by Ho and Stringfellow based on a modified VFF model, the solubility limit of InN in GaN is less than 5% at these growth temperatures (Fig. 2).[16] The sample discussed above is identified as A in the figure, corresponding to 37% indium. The phase diagram predicts spinodal decomposition, resulting in $In_{0.95}Ga_{0.05}N$ and $In_{0.05}Ga_{0.95}N$ (corresponding to the solid lines). Our data shown in Fig. 1 are in good agreement with the phase diagram. However, we still see the $In_{0.37}Ga_{0.63}N$ peak, since phase separation was incomplete due to kinetic limitations.

To investigate the role of growth temperature on phase separation, we grew several films at lower temperatures (650–675 °C) on *A*-plane sapphire. In this study, we examined a number of thick InGaN films with indium content less than 35%. Although XRD data did not show any InN related peaks, we observed chemical inhomogeneity in these films,

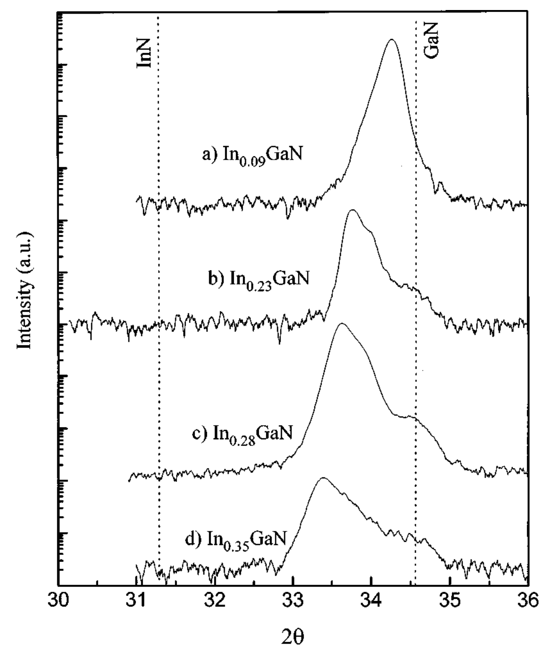


FIG. 3. X-ray diffraction patterns from the as-grown InGaN films of different compositions.

especially in those with high indium concentrations. Figure 3 shows $\theta-2\theta$ XRD patterns near the (0002) Bragg reflections of some of the InGaN films grown at these lower temperatures. Figure 3(a) shows a single peak corresponding to $In_{0.09}Ga_{0.91}N$. However, with an increase in indium composition, the (0002) Bragg reflection is broadened, indicating that the InGaN alloy is not chemically homogeneous. Such inhomogeneity could also be inferred from the SAD pattern shown in Fig. 1(b), where the diffraction spots corresponding to $In_{0.37}Ga_{0.63}N$ (the outer set) are seen to be diffused and split, rather than being sharp. Similar findings were reported by El-Masry *et al.* in the films grown by MOCVD.[20]

Compositional inhomogeneity observed in our films may be a result of one of three possible mechanisms. One mechanism is growth of InN precipitates, which may nucleate as a result of coalescence of In droplets on the surface during growth. In our SEM analysis, we do not observe any droplets or InN related peaks to support this mechanism. A second possibility is direct precipitation of InN from the bulk of the InGaN lattice by a nucleation and growth mechanism. This involves long-range diffusion and is strongly dependent on temperature and growth time. A third mechanism is spinodal decomposition, where phase separation occurs without nucleation, by ''up-hill'' diffusion. Although this is also dependent on temperature and growth time, the initial diffusion lengths can be much shorter, and therefore a more plausible mechanism at the relatively low temperatures used for growth of these films. At our growth temperature, the calculations predict that the alloy is metastable for compositions between 5% In and 20% In (where phase separation can only occur by nucleation and growth), and unstable for In$>$20% (where spinodal decomposition is expected) as seen from Fig. 2.

To understand this phase separation phenomenon further, annealing studies were carried out on two bulk InGaN

Downloaded 22 May 2002 to 128.197.57.187. Redistribution subject to AIP license or copyright, see http://ojps.aip.org/japo/japcr.jsp

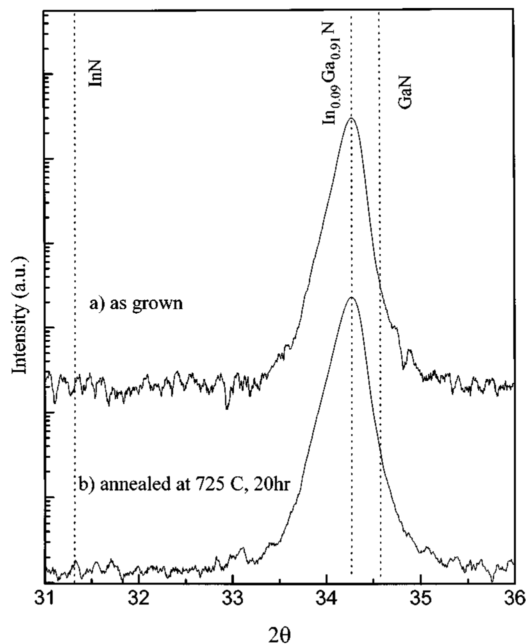


FIG. 4. X-ray $\theta-2\theta$ patterns from $In_{0.09}GaN$ film (a) as grown and (b) after annealing at 725 °C for 20 h.

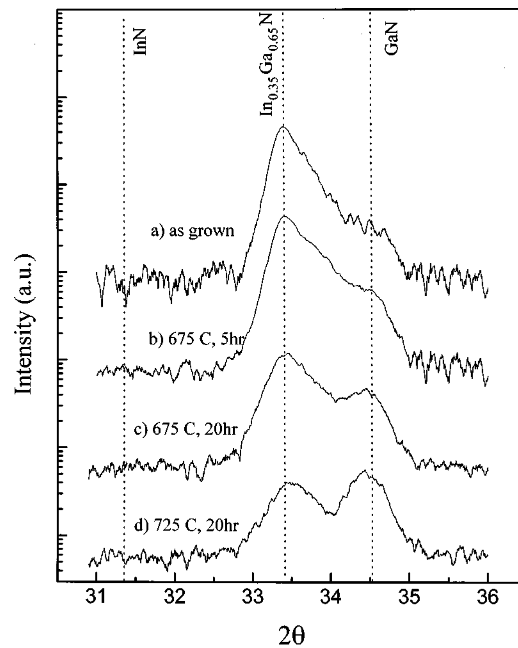


FIG. 5. X-ray $\theta-2\theta$ patterns from $In_{0.35}GaN$ film (a) as grown and after annealing (b) at 675 °C for 5 h, (c) at 675 °C for 20 h, and (d) at 725 °C for 20 h.

films shown in Fig. 2: sample B (with 9% indium) and sample C (with 35% indium). To minimize the film degradation, the annealing experiments were carried out at atmospheric pressure, in a nitrogen ambient. Figure 4 shows the XRD scans near the (0002) peak of sample B ($In_{0.09}Ga_{0.91}N$), which falls in the metastable region of the calculated phase diagram. There was no change in the film after annealing for 20 h at 725 °C. On the other hand, there were significant changes in the structure of sample C, whose composition is in the ''unstable'' region of the calculated phase diagram. Figure 5 shows the XRD scans near the (0002) peak of the film with 35% indium (sample C), annealed at various temperature–time conditions. Emergence of phase separated GaN can be clearly seen in the figure. After annealing for 20 h at 725 °C, the intensity of the GaN peak exceeded even that of $In_{0.37}Ga_{0.63}N$, which is strong evidence of phase separation, possibly by spinodal decomposition. The absence of a corresponding InN peak at $2\theta=31.35°$ is attributed to InN evaporation. This was confirmed by SEM data, which showed a roughened surface and a decrease in the film thickness. Spinodal decomposition occurs by up-hill diffusion and can be initiated by small local fluctuations in composition. In the case of sample B, phase separation is predicted to occur by nucleation and growth, which usually requires diffusion over longer distances and hence takes a much longer time (at a particular temperature). These results are in excellent agreement with the phase diagram proposed by Ho and Stringfellow.[16]

## B. Long-range atomic ordering

In general, the majority of the III–V ternary and quaternary alloys are predicted to be thermodynamically unstable at a low growth temperature and show a tendency towards clustering and phase separation.[1,12–14] Thus, atomic ordering is usually not expected to occur. However, such a phenomenon was theoretically predicted[23] and observed in many III–V alloys.[2,4,24,25] Our group also reported long-range atomic ordering in AlGaN alloys.[26] We have, for the first time, found similar behavior in InGaN alloys. In a random InGaN alloy, the structure factor of (000*l*) planes is zero where *l* is odd. In an ordered alloy on the other hand, indium atoms occupy certain lattice sites preferentially, resulting in a change in the structure factors of corresponding lattice planes. Indium atoms preferentially occupying lattice sites in alternating basal planes result in nonzero structure factors for (000*l*) planes. Figure 6 is a XRD scan from $In_{0.09}Ga_{0.91}N$ film, which clearly shows the presence of the (0001) peak, indicating ordering of the In atoms in the alloy. Xiao *et al.* have observed a (0001) XRD peak in pure GaN due to defect ordering, but the (0001)/(0002) ratio in this

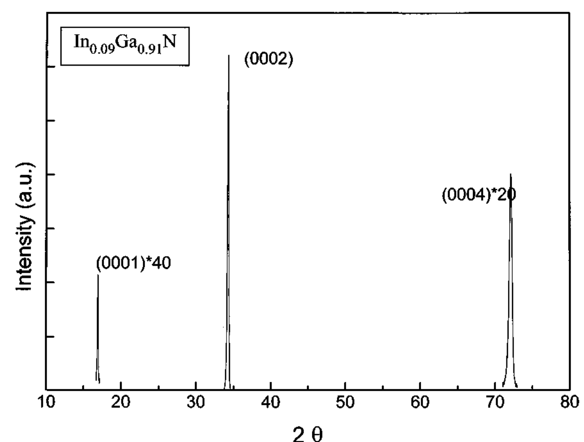


FIG. 6. X-ray $\theta-2\theta$ patterns from $In_{0.09}GaN$ film showing the presence of the (0001) peak, indicating ordering.

Downloaded 22 May 2002 to 128.197.57.187. Redistribution subject to AIP license or copyright, see http://ojps.aip.org/japo/japcr.jsp

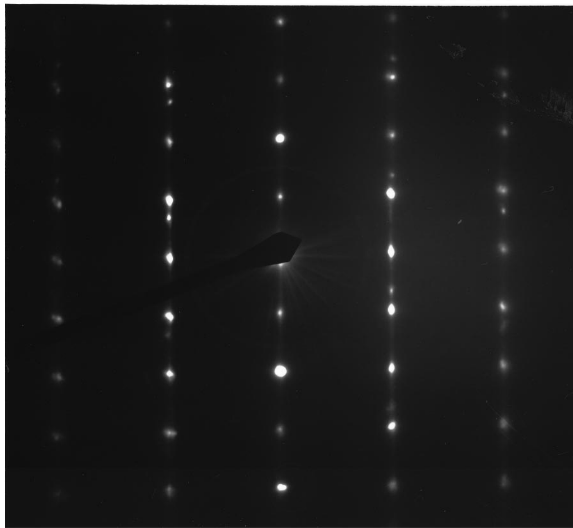

FIG. 7. Cross-sectional SAD pattern along the [11-20] zone axis from the $In_{0.09}Ga_{0.91}N$ film, showing the presence of (0001) spots as well as streaking in the [0001] direction.

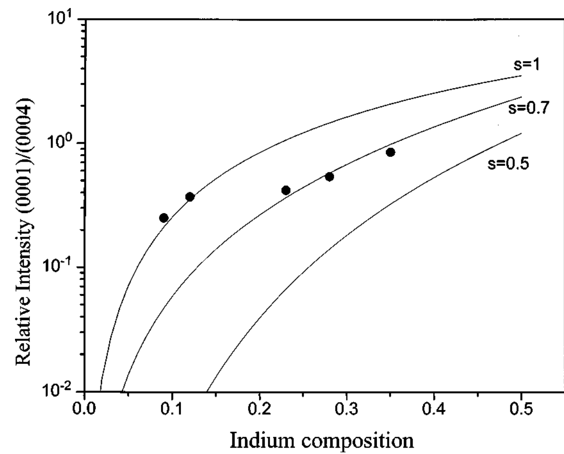


FIG. 8. Relative intensity of (0001) and (0004) peaks plotted as a function of indium composition, for different degrees of ordering, $S$. The solid circles indicate the experimental data.

case was only $10^{-6}$,[27] which is about 4 orders of magnitude less than what we observe in InGaN films, implying that the ordering is not defect related. Similar XRD data were obtained in all InGaN films investigated. Figure 7 is a SAD pattern obtained in TEM studies from an InGaN film with 35% indium, taken along the [11-20] zone axis. Although the pattern also shows the presence of (0001) spots, this cannot be conclusively attributed to ordering since similar features could be observed even in pure GaN due to double diffraction. However, very prominent streaking of diffraction spots was observed in the [0001] direction (Fig. 7), which is an indication of atomic ordering. Such streaks in the SAD pattern were observed before in AlGaAs alloys by Kuan *et al.*,[25] who attributed them to partial ordering and ''anti-phase boundaries,'' in the growth direction.

To obtain an accurate estimate of the degree of ordering in these films, the intensities of (0001) and (0004) Bragg reflections were compared to account for any possible variations in beam intensities, film thickness, and orientation effects. XRD results showed that the ratio of (0001) and (0004) peak intensities increased with composition of indium in the films. These experimental results were compared with the calculated intensity ratios for perfectly ordered alloys. In general, the intensity of a $(hkl)$ Bragg reflection is given by[28]

$$I_{(hkil)}=|F_{hkil}|^2\left(\frac{1+\cos^2 2\theta\cos^2 2\alpha}{\sin\theta\cos\theta}\right)\times\left(\frac{1}{\sin\theta}\right)A(\theta)\exp(-2M), \quad (1)$$

where $\mathbf{F}_{hkil}$ is the structure factor for the $(hkil)$ plane, the term in the brackets is the Lorentz polarization parameter, $A(\theta)$ is the absorption factor, the exponential term is the Debye–Waller temperature factor and the $(1/\sin\theta)$ term accounts for the differences in the film volume exposed at different angles. In the equation, $\theta$ is the Bragg angle of the $(hkil)$ reflection and $\alpha$ is the Bragg angle of the monochromator [13.63° in this case, for the Ge (111) plane we used]. The structure factor $F_{000l}$ is calculated from the atomic scattering factors of the constituent atoms. Group III atom positions in the unit cell are taken to be at (0, 0, 0) and (1/3, 2/3, $\frac{1}{2}$) and nitrogen positions at (0, 0, 3/8) and (1/3, 2/3, 7/8). The long-range ordering parameter, $S$ is given by the relation

$$S=\frac{r_A-x}{1-x}, \quad (2)$$

where $\mathbf{r}_A$ is the fraction of $A$ sites occupied by the atoms of type $A$ and $x$ is the mole fraction of $A$ in the compound. Therefore, in a perfectly ordered $(S=1)$ $In_xGa_{1-x}N$ alloys, $\mathbf{r}_A=1$. In this case, all the indium atoms $(2x)$ are assumed to be on the (0002) plane and the rest of the sites on (0002) as well as all the sites on (0001) plane to be taken up by Ga atoms. Now, the structure factor for the $(000l)$ plane, $F_{000l}$, is given by

$$\begin{aligned}F_{000l}=&\{2x(1-r_{\mathrm{In}})f^l_{\mathrm{In}}+[1-2x(1-r_{\mathrm{In}})]f^l_{\mathrm{Ga}}\}\\&\times i\ \exp[2\Pi i(0)]+[2r_{\mathrm{In}}x.f^l_{\mathrm{In}}+(1-2r_{\mathrm{In}}x).f^l_{\mathrm{Ga}}]\\&.\exp[2\Pi i(l/2)]+f^l_N.\{\exp[2\Pi i(3l/8)]\\&+\exp[2\Pi i(7l/8)]\},\end{aligned} \quad (3)$$

where, $f^l$ is the atomic structure factor of the particular atom at $\theta$ corresponding to the $(000l)$ diffraction peak.

The ratio $I_{0001}/I_{0004}$ is calculated from the above expressions, using tabulated values for the various structure factors.[28] The absorption factor was calculated for the two $\theta$ values, by estimating mass absorption coefficients for different indium compositions and taking the film thickness to be 0.5 $\mu$m. The ratio of Debye–Waller temperature factors for the two peaks was calculated to be 1.05, taking the value of the Debye temperature of 770 °C for GaN.[29] The curves in Fig. 8 show the variation in the calculated relative intensity of (0001)/(0004), as a function of composition for different ordering parameters. The experimental data points shown are for samples grown under similar conditions of temperature, growth rate, and final thickness. The figure shows that at

Downloaded 22 May 2002 to 128.197.57.187. Redistribution subject to AIP license or copyright, see http://ojps.aip.org/japo/japcr.jsp

lower indium compositions, complete ordering occurs ($S=1$). At higher indium concentrations, the films exhibit partial ordering ($S\sim 0.7$).

Srivastava and co-workers[23] performed first principle local density total minimization calculations for both ordered and disordered models for bulk GaInP and predicted that certain ordered phases could be thermodynamically stable at low temperatures. The stability of these ordered phases is due to the reduction of strain in the ordered versus disordered phases. We believe that the driving force for ordering in the InGaN system is the lattice strain in the alloy due to differences in In–N and Ga–N bond lengths. Since the ordered phases can simultaneously accommodate two different bond lengths in the alloy in a coherent fashion, they introduce less strain than would be present in a random alloy. This is consistent with the relatively smaller degree of ordering observed in the samples with high indium composition, where strain is already partially relieved by phase separation. We believe that this competition between ordering and phase separation is the reason why the data of Fig. 8 do not follow the kinematical scattering theory. In AlGaN alloys in which phase separation was not observed, the data are qualitatively consistent with the theory.[26] The ordering observed in our films closely resembles the Cu–Pt type ordering observed earlier in other III–V compounds with zinc-blende structure.[4,5] In these compounds, ordering is characterized by $\frac{1}{2}\{111\}$ superlattice reflections, which are structurally similar to (0001) superlattice reflections we observe in our wurtzite films. Total energy calculations done in other III–V compounds[30] suggest that the Cu–Pt type ordered phase is thermodynamically unstable in bulk. However, once ordering is induced at the surface during growth, it is retained during further growth due to kinetic limitations.

We also performed post-growth annealing experiments in the films that do not show phase separation, to study the stability of these ordered phases. Annealing of $In_{0.09}Ga_{0.91}N$ film (up to 725 °C for 20 h) did not result in any significant changes. The relative intensities of (0001) and (0004), within experimental errors, remained the same. Based on this evidence, we believe that the ordered phase in the InGaN system is fairly stable in the bulk. This is in contrast to other III–V compounds investigated, in which case, post-growth annealing experiments indicated that the ordered phase is unstable in the bulk.[5,31] However, it should be noted that the InGaN alloys are more refractory materials than the those investigated previously.

We correlated the long-range ordering parameter, $S$, to the growth parameters in various films. Apart from the composition, we found that $S$ depends strongly on growth rate. Figure 9 shows the variation of the degree of ordering with the growth rate for the films of the same composition (28% In) grown under similar conditions. It is clear that the order parameter $S$ increases monotonically with the growth rate in the films studied. This, we believe, results from the relatively slow growth of the InGaN alloys in general. The slow arrival of atoms at the surface provides sufficient time for surface ordering to occur. Once the surface gets trapped in the bulk, it wants to disorder. However, disordering can occur effectively only in the near-surface region of the film. The absence of disordering in the bulk alloy is supported by the stability of the ordered phase to annealing up to temperatures of 725 °C for 20 hours. Thus for faster growth rates, the time spent in the near surface region is smaller, allowing for a smaller extent of disordering to occur (effectively ''freezing'' the ordered phase) and leading to a larger value of $S$. This strongly supports the contention that ordering is a surface phenomenon. This trend is in apparent contradiction to the observations in cubic III–V compounds,[1] which show a decrease in ordering with growth rate. We believe that this is due to much faster growth rates used in these materials, which does not allow sufficient time for surface ordering to occur.

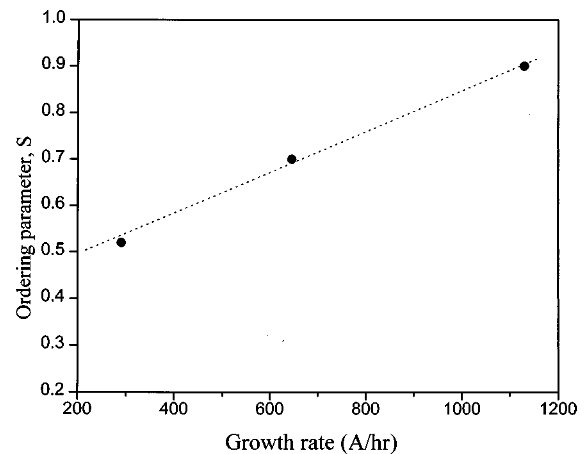


FIG. 9. Variation in long-range order parameter ($S$) with growth rate, in InGaN films grown under the same conditions and with the same composition.

## IV. CONCLUSIONS

In conclusion we studied phase separation and ordering phenomena in InGaN alloys produced by MBE. Films grown at substrate temperatures of 700–750 °C with indium concentration higher than 35% generally show phase separation in agreement with thermodynamic predictions of Ho and Stringfellow. Films grown at lower substrate temperatures (650–675 °C) show compositional inhomogeneity if the indium content is larger than 25%. Upon annealing to 725 °C of such films with high In content, the material undergoes similar phase separation as those grown at the same temperatures. The InGaN films were also found to show long-range atomic ordering similar to the Cu–Pt type ordering in zinc–blende structures. The ordering parameter was found to increase with the growth rates of the films, a result which is consistent with the notion that ordering is induced at the surface of the growing films where it is thermodynamically stable and is then subsequently ''frozen in'' during further growth. Preliminary annealing studies show that the ordered phase is fairly stable. Phase separation was found to be maximum in films with high In content ($>25\%$), while ordering is maximum in films with small In content ($<10\%$). This competition between the two phenomena is consistent with the proposal that lattice strain is the driving force for both.

Downloaded 22 May 2002 to 128.197.57.187. Redistribution subject to AIP license or copyright, see http://ojps.aip.org/japo/japcr.jsp

Optimization of these phenomena could lead to materials with desirable inhomogeneities for optoelectronic devices.

## ACKNOWLEDGMENTS

The authors would like to thank Raj Singh and E. Iliopoulos for useful discussions. This work was partially supported by DARPA (Contract No. 972-96-3-0014) and the Center for Photonics Research at Boston University.

[1] A. Zunger and S. Mahajan, in *Handbook on Semiconductors*, edited by S. Mahajan (North-Holland, Amsterdam, 1994), Vol. 3.
[2] S. Mahajan, Mater. Sci. Eng., B **30**, 187 (1995).
[3] K. Lee, B. A. Philips, R. S. McFadden, and S. Mahajan, Mater. Sci. Eng., B **32**, 231 (1995).
[4] B. A. Philips, A. G. Norman, T. Y. Seong, S. Mahajan, G. R. Booker, M. Skowronski, J. P. Harbison, and V. G. Keramidas, J. Cryst. Growth **140**, 249 (1994).
[5] A. G. Norman, T-Y. Seong, I. T. Ferguson, G. R. Booker, and B. A. Joyce, Semicond. Sci. Technol. **8**, 9 (1993).
[6] S. Nakamura, T. Mukai, and M. Senoh, Appl. Phys. Lett. **84**, 1687 (1994).
[7] S. Nakamura, M. Senoh, S. Nagahama, N. Isawa, T. Yamada, T. Matsushita, H. Kiyoku, and Y. Sugimoto, Jpn. J. Appl. Phys., Part 2 **35**, L74 (1996).
[8] I. Akasaki, S. Sota, H. Sakai, T. Tanaka, M. Koike, and H. Amano, Electron. Lett. **32**, 1105 (1996).
[9] S. Nakamura *et al.*, Appl. Phys. Lett. **72**, 211 (1998).
[10] T. Matsuoka, T. Sakai, and A. Katsui, Optoelectron., Devices Technol. **5**, 53 (1990).
[11] E. L. Piner, F. G. McIntosh, J. C. Roberts, K. S. Boutros, M. E. Aumer, V. A. Joshkin, N. A. El-Masry, S. M. Bedair, and S. X. Liu, Mater. Res. Soc. Symp. Proc. **449**, 85 (1997).
[12] G. B. Stringfellow, J. Cryst. Growth **58**, 194 (1982).
[13] M. B. Panish and M. Ilegems, in *Progress in Solid State Chemistry*, edited by M. Reiss and J. O. McCaldin (Oergamon, New York, 1972), p. 39.
[14] J. L. Martins and A. Zunger, Phys. Rev. B **30**, 6217 (1984).
[15] R. Singh, D. Doppalapudi, T. D. Moustakas, and L. T. Romano, Appl. Phys. Lett. **70**, 1089 (1997).
[16] I. H. Ho and G. B. Stringfellow, Mater. Res. Soc. Symp. Proc. **449**, 871 (1997).
[17] R. Singh and T. D. Moustakas, Mater. Res. Soc. Symp. Proc. **395**, 163 (1996).
[18] R. Singh, W. D. Herzog, D. Doppalapudi, M. S. Unlu, B. B. Goldberg, and T. D. Moustakas, Mater. Res. Soc. Symp. Proc. **449**, 185 (1997).
[19] A. Wakahara, T. Tokuda, X. Dang, S. Noda, and A. Sasaki, Appl. Phys. Lett. **71**, 906 (1997).
[20] N. A. El-Masry, E. L. Piner, S. X. Liu, and S. M. Bedair, Appl. Phys. Lett. **72**, 40 (1998).
[21] S. Chichibu, T. Azuhata, T. Sota, and S. Nakamura, Appl. Phys. Lett. **70**, 2822 (1997).
[22] T. D. Moustakas, T. Lei, and R. J. Molnar, Physica B **185**, 36 (1993).
[23] G. P. Srivastava, J. L. Martins, and A. Zunger, Phys. Rev. B **31**, 2521 (1985).
[24] T. Suzuki, A. Gomyo, and S. Iijima, J. Cryst. Growth **93**, 396 (1988).
[25] T. S. Kuan, T. F. Kuech, W. I. Wang, and E. L. Wilkie, Phys. Rev. Lett. **54**, 201 (1985).
[26] D. Korakakis, K. F. Ludwig, Jr., and T. D. Moustakas, Appl. Phys. Lett. **71**, 72 (1997).
[27] H. Z. Xiao, N. E. Lee, R. C. Powell, Z. Ma, L. J. Chou, L. H. Allen, J. E. Green, and A. Rockett, J. Appl. Phys. **76**, 8195 (1994).
[28] B. D. Cullity, *Elements of X-ray Diffraction* (Addison-Wesley, Reading, MA, 1978).
[29] A. Dimitriev, MRS Internet J. Nitride Semicond. Res. **1**, 46 (1996).
[30] J. E. Bernard, R. G. Dandrea, L. G. Ferreira, S. Froyen, S-H. Wei, and A. Zunger, Appl. Phys. Lett. **56**, 731 (1990).
[31] W. E. Plano, D. W. Nam, J. S. Major, Jr., K. C. Hsieh, and N. Holonyak, Jr., Appl. Phys. Lett. **53**, 2537 (1988).

Downloaded 22 May 2002 to 128.197.57.187. Redistribution subject to AIP license or copyright, see http://ojps.aip.org/japo/japcr.jsp